Population Kinetics of a Repetitively-Pulsed Nanosecond Discharge

by

Benjamin T. Yee

A dissertation submitted in partial fulfillment
of the requirements for the degree of
Doctor of Philosophy
(Nuclear Engineering & Radiological Sciences)
in the University of Michigan
2013

Doctoral Committee:

Associate Professor John E. Foster, Chair
Doctor Edward V. Barnat, Sandia National Laboratories
Doctor Isaiah M. Blankson, National Aeronautics and Space Administration
Professor Augustus Evrard
Professor Mark J. Kushner

I would like to dedicate this dissertation to someone else.

ACKNOWLEDGMENTS

Who is this?

Preface

This is a dissertation about something; I really hope it's good.

TABLE OF CONTENTS

LIST OF FIGURES

LIST OF TABLES

LIST OF APPENDICES

LIST OF ABBREVIATIONS

RPND repetitively-pulsed nanosecond discharge

APP atmospheric-pressure plasma

VFP Vlasov-Fokker-Planck

EEDF electron energy distribution function

FIW fast ionization wave

LAS laser-absorption spectroscopy

LCIF laser collision-induced fluorescence

CHAPTER 1

Introduction

1.1 Overview

1.1.1 Motivation

Plasmas, commonly called the fourth state of matter, are a gas where a significant fraction of the neutral atoms or molecules have been split into pairs of electrons and positive ions. Initially, a curiosity of the laboratory, they have become a critical part of every day life. The electrically charged nature of plasmas makes them a practical means by which to convert electrical energy into light, chemical reactions, kinetic energy, or even nuclear reactions. From an applications perspective, they are indisposable in lighting, semiconductor manufacturing, plastic processing, and space propulsion. On a more broad scale, virtually all observable light in the universe is the result of a plasma in some form or another.

Some exceptions aside, only three things are required to create a plasma: a gas, an energy source, and a means of transferring the energy to the gas. In man-made applications, the energy source is typically electricity, and the simplest transfer mechanism are two electrodes placed on either side of the gas. This results in an electric field in the gap between the electrodes, as seen in figure 1.1. The field accelerates a single seed electron in the gas (often created by background cosmic radiation) until it collides with a neutral particle. The electron, having acquired a fair amount of energy, knocks a second electron loose from the particle, leaving behind a relatively heavy and immobile ion. Subsequently, both the first

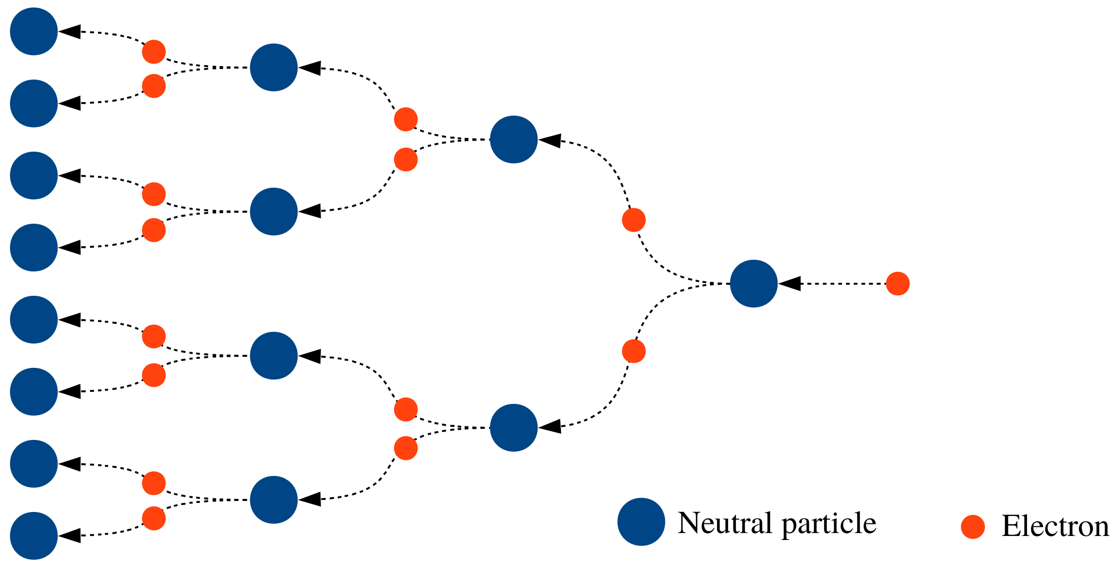

Figure 1.1: A simplified depiction of the avalanche breakdown process in a gas.

and second electron are now accelerated by the electric field. Again, they collide with two more neutral atoms, creating two new electrons. As long as the electric field persists, the number of electron and ion pairs increases exponentially. This process is generally referred to as an avalanche.

Despite this relatively simple recipe, the physical characteristics can vary greatly depending on what gas is used, what pressure it is at, what voltage is used, whether the electricity is applied constantly or varied over time, what kind of electrodes are used, etc. As a result, man-made plasmas are generally produced under very specific conditions. For example, a plasma etcher used in semiconductor manufacturing may need to operate operate at pressures that are one-thousandth of atmospheric pressure with ultra-pure (99.9999%) gases.

Plasmas like those which occur in plasma etchers, feature ions and neutral gas particles with temperatures that are below 1,000 K, or roughly 1,340· F. Though this temperature is relatively high compared to room temperature, it is well below the temperature of the electrons which may be in excess of 20,000 K. Plasmas which exhibit this disparity in temperatures are often called nonequilibrium or "low-temperature" plasmas.

Conversely, there exists another class of plasmas where the electrons, ions, and neutral particles are all at the same temperature. These are called thermal plasmas. Generally speaking, the closer the gas pressure is to atmosphere, the more thermal a plasma is. Additionally, the temperatures in a thermal plasma can be quite high and, in many cases, can easily melt most metals. For example, the arc of an arc welder is a thermal plasma. Similar high temperature plasmas, have a number of other applications which include a variety of high-intensity lamps, metal cutting, and surface coating.

There are, however, a number of applications which would benefit from operation at higher pressures, but with low-temperature ions and neutrals so as to avoid heat damage. This has spurred a substantial amount of research on nonequilibrium atmospheric-pressure plasmas (APPS) in recent years. Ideally, such a plasma could be generated at or near atmospheric pressure with hot electrons, but minimal heating of surrounding gas. Though this field of research is still relatively young, it has produced a variety of new plasmas and capabilities. One of the more ubiquitous examples is use of plasmas to process the surface of plastics so that ink can adhere. Separately, nonequilibrium APPS are the technology which drives plasma televisions.

As mentioned, these applications promise to be the first of many for such plasmas. More recently, there have been innovative proposals to use these plasmas in water purification, wound sterilization, improved combustion engines, nanoparticle production, and more. However, each situation has its own challenges when it comes to the design and development of a plasma source, particularly at these elevated pressures. Particularly problematic is the tendency of APPS to develop instabilities which can cause them to rapidly transition to thermal plasmas in a matter of nanoseconds.

There exist a few ways of getting around these instabilities. One example is the dielectric-barrier discharge which passively regulates the amount of power which can be deposited into the plasma. Another example includes split-ring resonators which use natural feedback mechanisms to damp out potential instabilities. The technique considered here, referred to as the repetitively-pulsed nanosecond discharge, or RPND, uses high voltage pulses which are so short that the instability does not have time to develop. The RPND is a nonequilibrium plasma which can operate at pressures ranging from approximately 10^{-3}–10 atmospheres. At atmospheric pressure the RPND can produce a uniform plasma in volumes on the order of 10 mL. As the pressure is reduced, the plasma volume can reach the order of liters.

The importance of large-area, uniform, high-pressure plasmas such as the RPND was highlighted in the National Academies' most recent decadal survey of plasma science [1]. However, there is still much that is not know about such plasmas. From the same survey, it is said that "the full promise of APPS will be known only if they can be understood and managed based on fundamental scientific principles at two extremes–the nanoscopic kinetic level, where selective chemistry occurs, and the global stability level." It is this challenge, specifically the investigation of the nanoscopic kinetic level, which drives the research presented here.

1.1.2 History

Historically, the study of low-temperature APPS has been almost indistinguishable from the study of plasmas as a whole. However, this was not necessarily a matter of reasoned choice. Plasma generation at atmospheric-pressure obviates the need for an effective vacuum pump. Additionally, prior to the creation of large battery banks, early sources of electrical energy had relatively small capacities. This precluded the generation of thermal atmospheric plasmas which required large amounts of energy.

Indeed, the requirements for a low-temperature APP are sufficiently rudimentary that the first man-made one (and likely the first man-made plasma), was probably a spark generated by rubbing fur against amber. This is commonly attributed to Thales of Milêtus from around 600 B.C. Following Thales, electrical sparks came to intrigue many scientists including Gottfried Liebniz, Benjamin Franklin, and Charles Wheatstone. By the mid-1800s, Plücker, Geißler, and Hittorf began some of the first work on low-pressure plasmas though it was

Crookes who would later identify plasma as a separate state of matter. Later, J.J. Thomson's discovery of the electron and discretized charge in 1897 marked the beginning of modern plasma research.

By this time, the necessary tools and techniques existed to create steady plasmas in pure, rarified gases. The behaviors of which were dominated by the motion and interaction of the charged electrons and ions. Critically, the effects of the neutral particles were negligible, thus isolating the electrical properties of the plasma. These carefully controlled systems were ideal for basic studies of plasma behavior and were used to great effect by individuals such as Irving Langmuir and Lewi Tonks. In fact, many modern concepts in plasma physics can be traced back to their work.

In contrast, the pulsed APPS, characteristic of the earliest man-made plasmas, were easy to create, but notoriously difficult to work with. It could take them only a few nanoseconds to form, and less than a millisecond to decay away. For many years, there were simply no instruments capable of taking measurements this quickly. Furthermore, the neutral particles which were of no consequence in the low-pressure plasmas, could not be ignored. The neutral particles were present in such quantities that they could confound or obscure otherwise simple measurements.

As a consequence, there is still a great deal that is not known about about pulsed APPS, particularly lightning, streamers, and a type of plasma which Thomson referred to as a "luminous front." By the 1970s, this latter plasma had come to be called the fast ionization wave, or FIW. It was generated by a single voltage pulse lasting around 100 nanoseconds and peaking at 10s or 100s of kilovolts. For the right pressure and gas, the FIW could fill volumes of nearly 40 L with a relatively uniform plasma, but with little heating of the gas.

These properties were attractive for a number of uses, but the FIW faced a number of implementation-related challenges. The switches used to trigger the FIW could only operate up to 100 times each second. Unfortunately, the lifetime of a plasma at elevated pressures is relatively short, and the plasma generated by the FIW would decay away quickly after each pulse. This meant that the FIW-generated plasma had a relatively low duty cycle; the ratio of the time the plasma spends on to the time it spends off. This was disadvantageous for plasma-processing applications where low duty cycles are equivalent to long processing times. The low duty cycle also necessitated so-called preionization of the gas with UV lamps or a secondary plasma generator, adding to the cost and complexity of the system. Finally, the pulse generators used for FIWS were not considered reliable enough for long operational lifetimes.

Recent advances in solid-state switching technology has largely solved these issues. At present, switches exist which can reliably operate 100,00 times a second; sufficiently fast that the plasma duty cycle approaches 100%. This has the additional benefit of obviating the need for a preionization stage, as a sufficient number of electrons persist between pulses. The discharge produced by the use of these new switches is what we refer to as the RPND.

1.1.3 Questions

The large pedigree of pulsed plasma research belies the fact that they are still not well-understood. This remains especially true for RPNDS which present significant experimental challenges. A major component of this has to do with the time scales associated with the RPND. The formation of a RPND often requires no more than 10-20 nanoseconds. Very sensitive equipment is required in order to measure changes which occur during this period. Unfortunately, such equipment is particularly susceptible to the broadband electronic noise generated by the fast pulses. There is a plethora of other problems that can be traced back to topic of timing. For example, things like the length and insulators of detector cables can introduce substantial delays, and must be considered in order to synchronize different measurements.

Consequently, the majority of RPND studies focus on measurements after the discharge has occurred, when changes happen at a much slower rate. A great deal of information is available for this period of time, including chemical compositions, atomic densities, electron densities, gas temperatures, and more. While undoubtedly important, these measurements provide limited insight on what is happening *while* the plasma is forming. It is natural, then, to ask, what are the RPND plasma properties during formation?

Additionally, most studies have used a limited range of gases: oxygen, nitrogen, air, hydrogen, or some mixture thereof. The choice of these gases is deliberate and reflects specific applications in combustion and aerospace. However, the use of rare gases (such as helium) and rare gas mixtures has become popular because they provide for a wider range of stable operating conditions. Notably, it has been found that unique internal structures of rare gases can produce very different discharges. Given this, there is the question of how rare gas RPNDs compare to more conventional ones.

Finally, the persistence of the plasma between pulses makes the development of a RPND very different from a FIW. One reason for this is the large number of electrons that remain between pulses in the RPND. While these seed electrons are necessary for the discharge to develop, in too large a number they can shield out the applied pulse. This can have the detrimental effect of reducing the final plasma density. These competing effects have to be balanced in order to obtain an optimal result, and what is considered optimal can vary depending on the application. Therefore, one must ask how the properties of a RPND compare to a similar FIW and how they vary depending on the operating conditions.

1.1.4 Approach

The dissertation presented here represents my efforts to either answer or provide a foundation to answer these questions. In order to develop the appropriate context for this work, the next section will be a comprehensive review of the RPND literature. It begins with the first reported pulsed APPS and concludes with contemporary studies.

The following two chapters set the basis for the experimental and numerical studies. Chapter 2 presents the theory necessary to understand RPNDS from basic gaseous discharges to cathode-directed streamers. Subsequently, chapter 3 describes the design of the helium

RPND discharge apparatus used for the experimental studies and as the basis for the simulations. Also included in this chapter are several measurements of the basic discharge properties.

Chapters 4 through 6 provide more detailed measurements and analysis of the RPND dynamics. In chapter 4, the measurements of the helium metastables in a RPND are presented and analyzed as a function of pressure an axial location in the discharge apparatus. Chapter 5 presents and analyzes similar measurements of the spontaneous plasma emissions. Finally, chapter 6 discusses the development of a global model for a helium plasma and its use with the experimental data to infer the plasma properties of the RPND. The dissertation concludes with a summary of the results and suggestions for further avenues of research.

1.2 Literature Review

RPNDs are only a recent invention which resulted from advances in fast-switching semiconductors. However, the physics of their formation is related to a much more broad category of plasmas which includes lightning, streamers, and even some transient phenomena in DC glows [2]. These plasmas are unique in that their spatial structure develops at speeds much faster than can be accounted for by the conventional Townsend mechanism. Loeb refers to this phenomena as "ionizing waves of potential gradient." [1].

1.2.1 Early History of Pulsed Discharges

In 1835 (as reported by Thomson [3]), Charles Wheatstone attempted to measure what he thought to be the speed of electricity between two electrodes, connected by a vacuum tube, six feet in length [4]. It is now known that he was actually measuring the speed with which a plasma formed between the two electrodes. He accomplished this by the use of a rotating

[1]It should be noted that the phrase wave does not indicate any kind of periodic motion or spatial arrangement. Simply put, it describes a boundary which separates ionized and unionized gas which travels from one electrode to another.

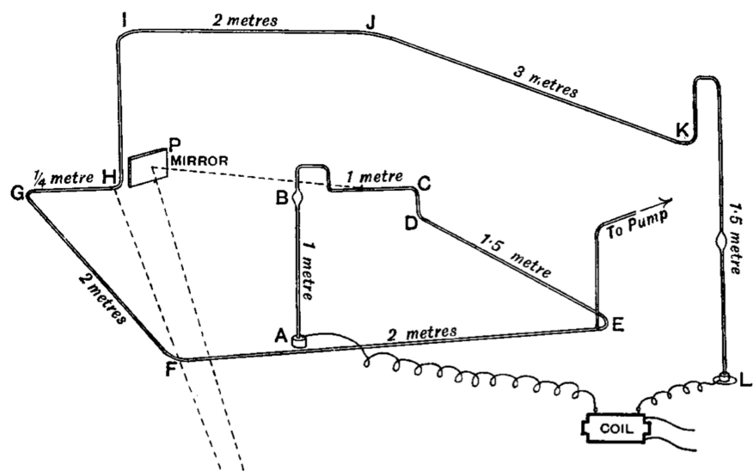

Figure 1.2: A sketch of J.J. Thomson's early experiments on pulsed plasmas in long vacuum tubes.

mirror which allowed him to see images of two sections of the tube, slightly displaced. The displacement between the images was proportional to the speed with which the plasma traveled between them. Wheatsone estimated this speed to be at least 8×10^7 cm/s.

Interestingly, von Zahn later noted that this was *not* the speed of the emitting particles [5]. That is, even though the visible light crossed the electrode gap at a high speed, the particles did not.

Later, Thomson revisited this work with an improved apparatus [3]. This included a tube that was now 15 m in length and five mm in diameter, as seen in figure 1.2. Also using the rotating mirror apparatus, Thomson was able to greatly improve on the estimates of Wheatstone. He estimated that the so-called "luminous front" had a speed that was more than 1.5×10^{10} cm/s, or in excess of half of the speed of light. Furthermore, Thomson determined that the luminous front always appeared to travel from the positively pulsed electrode (anode) to the ground electrode (cathode).

The study of these luminous fronts was revisited by several researchers in the wake of Thomson [6–8], but their attempts to duplicate the measured speeds were met with varied success. In 1930, Beams confirmed definitively confirmed those of Thomson. He also discovered that the front always traveled from the electrode with the highest absolute potential, to the lowest one. In other words, it could be anode *or* cathode directed, depending on the magnitude of their potentials relative to ground. Beams hypothesized that the rapid motion of the front was a result of a self-propagating region of high space charge, quote:

> In the neighborhood of the electrode . . . the field is very high and intense ionization should take place. This ionization due to the large difference in mobilities of positive ions, negative ions and electrons respectively should result in the establishment of a space charge. This space charge, once formed near the high potential electrode Q must move down the tube regardless of the polarity of the applied potential because of the changes it produces in the field near its edges.

At about the same time, Schonland and Collens reported on their observations of lightning [9]. Though the general structure and length scale of lightning is substantially different from the luminous fronts observed by Beams and Thomson, the two phenomena would later prove to be very similar. In their work Schonland and Collens noted that lightning would usually occur in a two-step process. Based on the images they obtained, they suggested that the leader was generated by a relatively small "dart" with a mean vertical velocity of 7.2×10^8 cm/s. The dart moved in a random manner, changing directions at random intervals, but always moving toward the ground.

The second step began when this dart reached the ground. Once there, a bright return stroke would occur along the same path that the leader had traced out. In contrast to the leader stroke, the return stroke had a velocity of 5×10^9 cm/s. Schonland and Collens hesitantly attributed the leader stroke to an extended electron avalanche, and the return stroke to thermal ionization along the conductive path generated by the dart. However, calculations by Cravath and Loeb showed that the speeds of the proposed avalanche was inconsistent with the fields at the head of a lightning stroke [10]. Instead, they suggested that the dart was actually a moving region of space charge which locally accelerated electrons to ionizing energies. This was similar to the mechanism earlier proposed by Beams.

1.2.2 The Streamer Model

It was long known that sparks in air were similar to lightning. Advances in technology during the 1930's led to experiments which reinforced this similarity. In response to the measurements of Schonland and Collens; Snoddy, Beams, and Dietrich studied the breakdown of gas in a long tube with both positive and negative applied potentials [11]. Using an oscillograph, they observed both the leader and a return stroke in both cases. However, the propagation of the plasma wave toward the cathode required a source electrons ahead of the wave. The authors proposed that photoionization might provide these necessary electrons.

Around the same time, Flegler and Raether had come to a similar conclusion regarding the importance of photoionization. This led them to develop a more thorough theoretical model for these waves [12] which came to be known as the streamer theory. This was followed by a similar treatment by Loeb and Meek [13–15]. The streamer theory divided the initial plasma formation into two steps. In the first step, an electron avalanche is initiated between two electrodes. The avalanche travels toward the anode and leaves behind a region of positive space charge. In the second step, the return stroke begins at the anode and travels along the conductive path generated by the initial avalanche toward the cathode.

The streamer model proved relatively successful in describing the development of sparks and lightning. Theoretical estimates of the speed matched the velocity measurements that were acquired with photographs and oscillographs. Additionally, the theory was able to account for the halting manner in which lightning was formed as well as the constriction in space.

Following the initial work of Flegler, Raether, Loeb, and Meek, a number of researchers began to explore the boundary between the Townsend mechanism and the streamer mechanism. Most notable was Fisher and Bederson's work in 1951 [16], which was later extended to nitrogen [17] and argon [18]. These studies suggested that the streamer theory was incomplete. Furthermore, the reliance of the streamer theory on photoionization would later prove very contentious [19]. Finally, there was a whole class of discharges that it did not readily explain.

1.2.3 Diffuse Streamers

Per Chalmers [20], Rogowski and Buss [21, 22] observed a fast, diffuse, glow discharge immediately prior to the filaments of a streamer discharge. Allibone and Meek, noted similar diffuse discharges in air based on oscillographs and photographs [23–25]. However, the Boys apparatus which was employed in these studies (an ancestor to the modern streak camera) was unable to capture the evolution of the diffuse glow, given its large spatial extent.

This was first noted by Allibone who attempted to use Lichtenberg figures[2] to definitively capture this diffuse glow [26]. Later, Saxe and Meek used the recently invented photomultiplier tube to record the evolution of the light emissions in the brief, diffuse glow [27] as a function of space. Both studies agreed in the existence of the diffuse glow, despite some disagreement on the nature of its geometry and propagation.

By 1968 (according to Kunhardt and Byszewski [28]), Stankevich and Kalinin had provided the most firm evidence yet of a diffuse discharge in a dense gas [29]. This was later confirmed by experiments with a pulsed nanosecond discharge by Mesyats, Bychkov, and Kremnev [30]. In their analysis, they noted that photoionization could not play a role in such short-lived discharges and thus there was a need for extensions to the streamer model.

In addition to the diffuse discharge, Stankevich and Kalinin also noted the detection of x-rays with each pulse. This suggested the presence of high-energy electrons impinging on the surface of the electrodes, despite the high collisionality of the dense gas. Not only that, but the electron energies could even exceed what would be expected from the vacuum electric fields [31]. The eventual conclusion was that the electric field associated with the space charge at the head of the streamer produced very energetic electrons which deposited their energy far from the streamer tip [28, 32], allowing the streamer to spread out beyond

[2]Such figures directly exposed photographic emulsions to the electrical discharge. The developed image was a time-integrated representation of the discharge.

the diffusive region of the electrons.

It was based on the studies of the fast electrons in these discharges that Mesyats, Bychov, and Kremnev proposed the use of a fast electron beam for pumping high-pressure gas lasers. Similar work was conducted simultaneously by Fenstermacher et al. [33]. Later, Hunter [34], and Koval'chuk and Mesyats [35] proposed that such discharges be used for fast-closing switches. The need for a homogeneous plasmas in these applications prompted Palmer [36], and Levatter and Lin [37] to investigate the necessary conditions for uniformity. They concluded that the primary requirement for uniformity was a threshold value of fractional ionization.

1.2.4 Repetitively-Pulsed Nanosecond Discharges

The type of discharge originally studied by Babich, Loika, and Tarasova came to be known as the fast ionization wave (FIW). In the years following its discovery, a substantial effort was made to document the properties of the FIW over a wide range of conditions. In these studies, the wave velocity, current, and attenuation were the most frequently measured quantities. Much of this work is summarized in a review by Vasilyak [38]. Also reviewed are Slavin and Sopin's work which was the first to attempt a computation of the electron energy distribution function EEDF in FIWS [39].

The experimental measurements and computational work reported by Vasilyak were expanded on by a series of studies conducted at the Moscow Institute of Physics. These are reviewed by Starikovskaia et al. [40] and included measurements of the electron density, electric field, and energy coupling for FIWS in air, nitrogen, and hydrogen. The computational work by Starikoskaia and Starikovskii [41] still represents the most detailed study of the EEDF in nitrogen FIWS.

However, Starikovskaia et al. noted that the usefulness of FIWS were limited, in part, by their repetition rates. The power supplies for FIWS were capacitor banks, charged in parallel, and discharged in series (also referred to Marx banks). Unfortunately, the spark gaps used to trigger these capacitor banks would not operate above a few hundred Hz. This changed in the late 1990's with the development and commercialization of fast, solid-state switches. Specifically, with the fast ionization dynistor it was possible to achieve repetition rates of 100 kHz.

This led to a new class of repetitively-pulsed discharges, or the RPND. These discharges operated at sufficiently high rates such that charged particles would persist between pulses, significantly increasing the plasma duty cycle. The improved qualities of the RPND over the FIW inspired a number of novel, application-driven studies. This included:

- Plasma-assisted combustion [42–44]
- Magnetohydrodynamic energy bypass engines [44–46]
- Plasma actuators [47, 48]
- High-pressure xenon lamps [49]
- Plasma medicine [50, 51]
- Water treatment [52]

Though not specific to the RPND, Becker et al. [53] provide an extensive discussion of the potential uses for non-equilibrium air plasmas.

As a result, contemporary researchers have produced a wealth of literature on the operation of RPNDS. More recently, there have been detailed measurements of the gas temperatures [42, 54–60], chemical composition [56–58], electric fields [61–63], and energy coupling [42, 64]. Notably, these studies have been generally restricted to molecular gases; air, nitrogen, and occasionally, hydrogen.

The first such study was the work of Laroussi and Lu who examined a RPND excited in a stream of helium flowing from a tube into air [65, 66]. The resulting plasma had the appearance of a jet, emitted from the open end of the tube. Using fast photography they observed that the jet was actually a series of plasma "bullets" formed with each pulse. Measurements of the bullet velocities showed that their speed greatly exceed what would be expected purely from electrons drifting under the applied electric field. They described the bullet as a classic cathode-directed streamer propagated by photoionization.

The plasma bullets of Laroussi and Lu spawned a great deal of interest in RPND helium plasma jets[3] For example, Walsh et al. studied the atomic oxygen production for helium-oxygen mixtures with the use of emission spectroscopy and a global plasma chemistry model [69]. Urabe et al. employed a variety of laser diagnostics to measure the radial density profiles of helium metastable atoms and molecular nitrogen ions in a similar jet. This work was supported by a number of two-dimensional plasma simulations such as those by Naidis [70] and Breden, Miki, and Raja [71].

Simultaneously, there has been a decline in the study of FIWS, and relatively little on large-volume RPNDS. One of the most recent FIW studies was produced by Takashima et al. [72]. In it, the authors reported on FIWS in helium and nitrogen which were studied using capacitive probes and voltage-current characteristics. The results were compared to extensive two-dimensional fluid simulations and an analytic, one-dimensional drift model. In most cases, the measurements and simulations showed good agreement.

[3] A distinction should be made between plasma jets, excited by sinusoidal power supplies, similar to the well-known dielectric-barrier discharge [67], and those produced by nanosecond pulses. Differences between the two were reported by Walsh, Shi, and Kong [68].

CHAPTER 2

Theory

2.1 Plasmas

A volume containing some number of charged particles can be considered a plasma if it meets three conditions. The first requires that the motion of charged particles is primarily determined by the electric and magnetic fields of the volume rather than through collisions with neutral particles. This is classically expressed by the inequality

$$\sqrt{n_\mathrm{e} e^2/(\varepsilon_0 m_\mathrm{e})} < \nu, \tag{2.1}$$

where n_e is the electron density, e is the fundamental charge, ε_0 is the permittivity of free space, m_e is the mass of an electron, and ν is the electron-neutral collision frequency. The left-hand side term is called the electron plasma frequency, it the characteristic frequency at which a plasma oscillates in response to a perturbation.

For a sufficiently large number of particles, the behavior of the each species of the plasma can be described by a continuous probability distribution function. This function,$f_\alpha(\vec{r}, \vec{v}, t)$, describes the probability of finding a particle of species α, at position $\vec{r}$, The distribution function for a particle can be determined by the Vlasov-Fokker-Planck VFP equation,

$$\frac{\partial f_\alpha}{\partial t} + \vec{v_\alpha} \cdot \nabla f_\alpha + q_\alpha \left(\vec{E} + \vec{v_\alpha} \times \vec{B}\right) \cdot \nabla_\mathrm{v} f_\alpha = \left(\frac{\partial f_\alpha}{\partial t}\right)_\mathrm{coll}. \tag{2.2}$$

Here, $\vec{E}$ is the electric field, $\vec{B}$ is the magnetic field, and $\partial f_\alpha/(\partial t)_{\text{coll}}$ is a term representing all collisions. The VFP equation is coupled to Maxwell's equations in order to obtain a self-consistent description of the particle distribution and the resulting fields. In essence, this is the Boltzmann equation from statistical mechanics, however it now includes several changes. Vlasov replaced the original force term with the Lorentz equation, and Fokker and Planck introduced the collision operator on the right-hand side. This is coupled with Maxwell's equations for a solution of the electric and magnetic fields in the plasma.

In the absence of external fields and with only elastic collisions, the equation admits the famous Maxwell-Boltzmann equilibrium distribution,

$$f_\alpha(v) = n\left(\frac{m_\alpha}{2\pi k_{\mathrm{B}}T}\right)^{3/2}\exp\left(-\frac{m_\alpha v_\alpha^2}{2k_{\mathrm{B}}T}\right), \tag{2.3}$$

where n is the number of degrees of freedom, k_{B} is Boltzmann's constant, and T is the temperature. A species of particles which possesses a Boltzmann distribution is said to be in equilibrium. Likewise, two species with the same distribution are in equilibrium.

Aside from this, the VFP equation is notoriously difficult to solve. As a result, most plasma models use various moments of equation 2.2 where the velocity dependence has been integrated out. These moments are the basis for the two-fluid equations, the MHD formulation, and global models. We will show the first three moments following the notation of Lieberman and Lichtenberg [73]. For example, the first moment is the continuity equation,

$$\frac{\partial n_\alpha}{\partial t} + \nabla\cdot(n_\alpha\vec{u_\alpha}) = G_\alpha - L_\alpha, \tag{2.4}$$

where $\vec{u_\alpha}$ is the mean velocity of species α, G_α is its rate of gain, and L_α is the rate of loss. This equation can be interpreted as the rate of change in particle density for a particular volume of space.

Though the continuity equation is much simpler than the original VFP equation, it cannot be solved alone. The mean velocity, $\vec{u}$, is undefined. Typically, this leads to the second moment,

$$mn_\alpha\left[\frac{\partial\vec{u_\alpha}}{\partial t}(\vec{u_\alpha}\cdot\nabla)\right]=q_\alpha n_\alpha(\vec{E}+\vec{u_\alpha}\times\vec{B})-\nabla\cdot\vec{\Pi_\alpha}+\vec{f}_{\alpha,\mathrm{coll}} \tag{2.5}$$

where $\vec{\Pi_\alpha}$ is the pressure tensor, and $\vec{f}_{\alpha,c}$ is the rate of momentum transfer into species α. Again, any solution is stymied by the presence of a new a term, in this case, $\vec{\Pi_\alpha}$. At this point, an equation of state can be used to close the set of equations, in this case relating the pressure to the density. However, later work will benefit from one more moment.

Following the conservation of momentum, the energy conservation equation can be derived from the VFP equation,

$$\frac{\partial}{\partial t}\left(\frac{3}{2}p_\alpha\right)+\nabla\cdot\frac{3}{2}(p_\alpha\vec{u}_\alpha)+p_\alpha\nabla\cdot\vec{u}_\alpha+\nabla\cdot\vec{q}_\alpha=\frac{\partial}{\partial t}\left(\frac{3}{2}p_\alpha\right)\Big|_{\mathrm{coll}} \tag{2.6}$$

where p_α is the species pressure, q_α is the heat flow vector, and the right-hand side is the time rate of change in energy as a result of collisions. In our case, we only consider the flux into the volume (from the electric field) and the distribution of this field via rate constants. This is the basis for the global model.

2.2 Atomic Spectroscopy

Spectroscopy spans a large body of theory which cannot be adequately covered here. Given that the measurements are all for helium, we will limit ourselves to a simple description of atomic spectroscopy. An atom is made of positively charged nucleus and a number of negatively charged electrons which orbit this nucleus. In the unperturbed, or ground state, the electrons occupy orbitals determined by a full solution of the Schrodinger equation.

However, interactions with other particles or photons can excite one or more of the electrons into orbitals with higher potential energy. In most cases relevant to low temperature plasmas, only a single electron will be excited at any given time. Depending on which orbital the electron is excited to, it can transition to orbitals with lower potential energy by emitting a photon. These are typically called allowed transitions.

Each orbital in an atom can be described by four quantum numbers.

- n - The principal quantum number.
- l - Orbital angular momentum number.
- j - Total angular momentum.
- m_j - Total angular magnetic moment.

The Pauli exclusion principle restricts more than a single electron from occupying any given state defined by this series of numbers. Additionally, each set of numbers determines the potential energy possessed by an electron in that particular level.

Allowed transitions are determined by a series of selection rules. These selection rules can be summed up as the following:

- $\Delta S = 0$
- $\Delta L = \pm 1$

Though other transitions are possible (spin and dipole forbidden respectively), they tend to require an external perturbation in order to induce transition.

Figure shows the what is commonly called a Grotrian diagram for helium. In this diagram, the vertical axis represents the energy above the ground state, and the levels are arranged horizontally based on increasing L. Levels which are radiatively linked are connected by solid lines. As can be seen in this figure, only the levels having $S = 1$ are radiatively connected to the ground state. As a result, any helium atoms that are excited into the triplet manifold tend to stay there, accumulating in the metastable state, 2^3S.

Approaching 24 eV, the excited electron enters what is known as the continuum. The energy separation between states goes as n^{-2}, thus at large n the spacing becomes quite close and the states are almost indistinguishable. The levels are often referred to as Ryberg states. Above 24.69 eV, the electron becomes totally detached from the helium nucleus, and all that remains is a singly ionized helium atom.

Though the emissions of ions can be quite useful in some plasmas, we do not concern ourselves with them in either the measurements or models. 24.69 eV is the largest known ionization potential, and as a result, the number of ions and the emissions associated with them remain relatively small.

2.2.1 Spectral Lineshapes

It is tempting to think that the energy spacing can be calculated exactly, however there is always some variance about a central energy. This is called the spectral lineshape, and it effects both the energy of the emitted photon in radiative transitions, and the photons that an atom can absorb. Though these variations can be attributed to quantum mechanical effects, the actual result can derived from the so-called dipole approximation.

In this case, we envision a single electron oscillating about a large, heavy, positive charge. The full details of this derivation are covered in Siegman [74], however we'll address some of the most pertinent portions here. The response of a collection of atoms to an applied electric field can be expressed as a quantity known as the susceptibility. This is generally defined as

$$\tilde{\chi}(\omega) \equiv \frac{\tilde{P}(\omega)}{\varepsilon_0 \tilde{E}(\omega)} \tag{2.7}$$

where $\tilde{\chi}$ is the electric susceptibility, $\tilde{P}$ is the macroscopic polarization, $\tilde{E}$ is the applied electric field, and ω is the frequency of the applied field.

Natural Linewidth The electric susceptibility often possesses both a real and imaginary component. Physically, these respectively represent the reactive and absorptive component of the medium. Accounting for level-dependent effects, the standard susceptibility for an atomic transition can be written as

$$\tilde{\chi}_{\mathrm{at}}(\omega) = -j\frac{3}{4\pi^2}\frac{\Delta N\lambda^3\gamma_{\mathrm{rad}}}{\Delta\omega_{\mathrm{a}}}\frac{1}{1+2j(\omega-\omega_{\mathrm{a}})/\Delta\omega} \tag{2.8}$$

where ΔN represents the population difference between the upper and lower levels of the oscillator, λ is the transition wavelength, γ_{rad} is the natural radiative lifetime of the oscillator, $\Delta\omega_{\mathrm{a}}$ is the linewidth of the transition (for an unperturbed atom, this is simply γ_{rad}), and ω_{a} is the angular frequency of the transition or oscillator.

This equation is generally known as the complex lorentzian. Separated into its components it expresses both the absorptive and reactive properties of the atomic medium. It also clearly susceptible to fields that are displaced from ω_{a}. This is the finite linewidth associated with atomic emissions and absorption.

This linewidth affects each atom within the medium. Each atom will emit or absorb radiation with a probability described by this susceptibility. Consequently, this natural linewidth falls under the homogeneous category of line broadening.

Pressure Broadening Also included in this category is pressure broadening, or more fundamentally, dephasing.

2.2.2 Radiation Trapping

CHAPTER 3

Experiment

3.1 Discharge Apparatus

The discharge apparatus geometry was consistent with the design of a coaxial transmission line. This is similar to the design guidelines provided by Vasilyak [38]. The inner conductor is the plasma generated by the fast ionization wave. Surrounding that is a coaxial dielectric, in this case a quartz tube with 2.75" Conflat flanges on either side. Finally, surrounding the dielectric is the outer conductor or shield. In this case, the shield was an aluminum cylinder with slits of approximately 1.5" by 12" milled lengthwise. Figure **??** is a photograph of this discharge apparatus.

One flange of the quartz tube was held at ground potential, while the other flange was pulsed to approximately 7 kV. Given that the plasma undergoes significant decay between pulses, it is assumed that the impedance is almost infinite when the pulse is first applied, thus the actual voltage on the powered electrode is likely closer to 14 kV. The aluminum shield provides the ground connection for the ground electrode. The two were connected using a copper shim and a compressive shaft collar. The aluminum tube was connected to a second ground shield with a one inch copper braid. This second shield was made of copper and was separated by a teflon cylinder, with walls approximately 1" in thickness, from the powered electrode. Figure **??** is a schematic of the discharge apparatus.

Connected to the powered electrode was a Conflat nipple and an angled quartz window used in the LCIF experiments. A short, silicone-coated, high voltage wire connected the window flange to the central conductor of an HN connector. The HN connector was seated on a square copper plate, which was pressed against the shield using four 10-32 screws.

The HN connector was used to attach the transmission line from the high voltage pulser. Initial experiments attempted to use N connectors, however these were susceptible to breakdown in the air gap which separated the center conductor from the outer shield. The transmission line was approximately 15 m in length. Observations, consistent with calculations, indicated that this provided a window of approximately 140 ns in which to make measurements before the reflected pulse returned to the system and re-energized the plasma.

Attached grounded flange was a second quartz envelope that isolated the ground electrode from the pumping section of the apparatus. Connected to the second quartz envelope was a stainless steel tee, one side of which was connected to an angled quartz window used for the LCIF experiments. The other side of the tee was isolated with an alumina break from a series of Conflat fittings connected to a roughing pump. The roughing pump was connected with a shutoff valve, as well as two bypass lines with inline needle valves for flow regulation.

3.2 Measurement Conditions

LAS, emission, and coupling energy measurements were made at three different operating pressures. The operating pressures were: 0.3, 0.5, 1.0, 2.0, 3.0, 4.0, 8.0, and 16.0 Torr. Pressures below 10.0 Torr were measured with a capacitance manometer with a full scale range of 10.0 Torr, above this a capacitance manometer with a full scale range of 100.0 Torr was used.

Optical measurements were made at three locations along the axis of the discharge. The measurement location closest to the anode was separated from it by a distance of approximately six inches. Each other optical measurement location was moved further from the anode by an additional three inches.

For each operating condition, measurements were made of the voltage and current. The voltage measurement was made via an internal divider from the power supply. Current measurements were made using an back-current shunt located at a break in the outer shield of the transmission line. The back-current shunt can be seen in Figure **??**. It is composed of nine, low impedance, one ohm resistors, connected in parallel. Each side of the resistors were soldered to a piece of copper foil which was then soldered to the outer shield. A calibrated DC power supply was used to measure the resistance of the current shunt.

All measurements were made using a LeCroy Waverider oscilloscope with a bandwidth of 1 GHz. Connections were made using minimal lengths of RG 50/U cable. When necessary for timing purposes, the cable lengths were matched. Connections were made using minimal lengths of RG 50/U cable. When necessary for timing purposes, the cable lengths were matched. All measurements which required maximum bandwidth were made with a using external 50 ohm terminators.

3.3 Energy Coupling

For comparison to other discharges, estimates of the energy coupling were made using the current and voltage characteristics at each operating pressure.

3.4 Absorption Setup

The LAS setup was based upon the used of a distributed-feedback laser diode. Temperature and current control of the diode provided coarse and fine tuning, respectively, for the output frequency. It was found that it was unnecessary to adjust the temperature for the diode once the correct transition was found, therefore all tuning was accomplished using current tuning.

The laser diode was produced by Toptica Photonics (model #LD-1083-0070-DFB-1), and had a nominal operating power of 70 mW at a center wavelength of 1083 nm. The diode was held inside a Toptica DL-100 diode housing which contained an integral thermoelectric cooler and collimating optics. The operation of the diode was controlled by a Toptica DC 110 monitor, DCC 110 current control, DTC 110 temperature control, and SC 110 scan control.

A schematic of the optical layout for the absorption experiment can be seen in Figure **??**. Immediately after exiting the housing, the beam was passed through an optical isolator in order to prevent instabilities from back reflections. Next the beam was attenuated using a neutral density filter in order to keep its intensity below the saturation level for the transition. Following that, the beam passed through two apertures for alignment. Here, the beam was split by a partially reflecting mirror. Approximately 98% of the beam was allowed to pass through to a reference photodiode (Thorlabs DET300). After passing through the plasma, entered another aperture to limit near-coincident plasma emissions. The background emissions were further reduced using a long pass filter with a cutoff of 1000 nm. Finally, the beam was coupled into an optical fiber which connected to the detection electronics.

The transmitted laser light was detected with an InGaAs photodiode (Thorlabs DET410). The signal from the diode was often too small to detect, so the output of the signal photodiode was sent through a voltage amplifier (Femto HVA-200M-40-B). The light response of this system is limited by the photodiode which has a nominal rise time of five nanoseconds. The signal from the amplifier was terminated by a 50 ohm terminator and sensed by the aforementioned oscilloscope.

3.4.1 Acquisition Process

The actual acquisition process required a specific series of steps in order to properly account for all noise sources. In order to accommodate this process, a custom LabView script was used to automate the acquisition of the laser transmission spectra. Generally speaking, the signal can be described as

$$V_{\mathrm{total}} = V_{\mathrm{signal}} + V_{\mathrm{background}} + V_{\mathrm{plasma}}. \tag{3.1}$$

In order to remove the background signal, the acquisition scr

3.5 Emissions Setup

CHAPTER 4

Metastable Measurements

CHAPTER 5

Emission Measurements

CHAPTER 6

Modeling

CHAPTER 7

Conclusions

APPENDIX A

Millimeter-Wave Interferometry

$$e = mc^2 \tag{A.1}$$

APPENDIX B

Rotational Spectroscopy

BIBLIOGRAPHY

[1] Plasma 2010 Committee, Plasma Science Committee, and National Research Council. *Plasma Science: Advancing Knowledge in the National Interest*. Number 2007. The National Academies Press, Washington, D.C., 2007.

[2] L B Loeb. Ionizing Waves of Potential Gradient: Luminous pulses in electrical breakdown, with velocities a third that of light, have a common basis. *Science (New York, N.Y.)*, 148(3676):1417–26, June 1965.

[3] J J Thomson. *Notes on Recent Researches in Electricity and Magnetism*. Clarendon Press, Oxford, UK, 1893.

[4] C. Wheatstone. Versuche, die Geschwindigkeit der Elektricität und die Dauer des elektrischen Lichts zu messen. *Annalen der Physik und Chemie*, 110(3):464–480, 1835.

[5] W. v. Zahn. Spectralröhren mit longitudinaler Durchsicht. *Annalen der Physik und Chemie*, 244(12):675–675, 1879.

[6] John James. Die Abraham-Lemoinesche Methode zur Messung sehr kleiner Zeitintervalle und ihre Anwendung zur Bestimmung der Richtung und Geschwindigkeit der Entladung in Entladungsröhren. *Annalen der Physik*, 320(15):954–987, 1904.

[7] R. Whiddington. The Discharge of Electricity through Vacuum Tubes. *Nature*, 116(2918):506–509, October 1925.

[8] J. Beams. The Time Interval Between the Appearance of Spectrum Lines in Spark and in Condensed Discharges. *Physical Review*, 28(3):475–480, September 1926.

[9] B. F. J. Schonland and H. Collens. Development of the Lightning Discharge. *Nature*, 132(3332):407–408, September 1933.

[10] a. M. Cravath and L. B. Loeb. The Mechanism of the High Velocity of Propagation of Lightning Discharges. *Physics*, 6(4):125, 1935.

[11] L. Snoddy, J. Beams, and J. Dietrich. The Propagation of Potential in Discharge Tubes. *Physical Review*, 50(5):469–471, September 1936.

[12] E. Flegler and H. Raether. Der elektrische Durchschlag in Gasen nach Untersuchungen mit der Nebelkammer. *Zeitschrift f r Physik*, 99(9-10):635–642, September 1936.

[13] Leonard B. Loeb and John M. Meek. The Mechanism of Spark Discharge in Air at Atmospheric Pressure. I. *Journal of Applied Physics*, 11(6):438, June 1940.

[14] Leonard B. Loeb and J. M. Meek. The Mechanism of Spark Discharge in Air at Atmospheric Pressure. II. *Journal of Applied Physics*, 11(7):459, 1940.

[15] J. Meek. A Theory of Spark Discharge. *Physical Review*, 57(8):722–728, April 1940.

[16] L. Fisher and B. Bedderson. Formative Time Lags of Spark Breakdown in Air in Uniform Fields at Low Overvoltages. *Physical Review*, 81(1):109–114, January 1951.

[17] G. Kachickas and L. Fisher. Formative Time Lags of Uniform Field Breakdown in N2. *Physical Review*, 88(4):878–883, November 1952.

[18] G. Kachickas and L. Fisher. Formative Time Lags of Uniform Field Breakdown in Argon. *Physical Review*, 91(4):775–779, August 1953.

[19] EE Kunhardt and Y Tzeng. Development of an electron avalanche and its transition into streamers. *Physical review. A*, 38(3):1410–1421, August 1988.

[20] I D Chalmers. The transient glow discharge in nitrogen and dry air. *Journal of Physics D: Applied Physics*, 4(8):1147–1151, August 1971.

[21] W Rogowski, E. Flegler, and R. Tamm. Über Wanderwelle und Durchschlag. *Archiv für Elektrotechnik*, 18(5):479–512, September 1927.

[22] K. Buss. Der Stufendurchschlag. *Archiv für Elektrotechnik*, 26(4):266–272, April 1932.

[23] T E Allibone and J M Meek. The Development of the Spark Discharge. II. *Proceedings of the Royal Society A: Mathematical, Physical and Engineering Sciences*, 169(937):246–268, December 1938.

[24] T. E. Allibone and J. M. Meek. The Development of the Spark Discharge. *Proceedings of the Royal Society A: Mathematical, Physical and Engineering Sciences*, 166(924):97–126, May 1938.

[25] T E Allibone. The Mechanism of a Long Spark. *Journal of the Institute of Electrical Engineers*, 82(497):513–521, 1938.

[26] T E Allibone. Development of the Spark Discharge. *Nature*, 161(4103):970–971, June 1948.

[27] R F Saxe and J M Meek. Development of Spark Discharges. *Nature*, 162(4111):263–264, August 1948.

[28] E Kunhardt and W Byszewski. Development of overvoltage breakdown at high gas pressure. *Physical Review A*, 21(6):2069–2077, June 1980.

[29] Yu. L. Stankevich and V. G. Kalinin. Fast Electrons and X-Ray Radiation during the Initial Stage of Growth of a Pulsed Spark Discharge in Air. *Soviet Physics Doklady*, 12, 1968.

[30] Gennadii A Mesyats, Yu I Bychkov, and V V Kremnev. Pulsed nanosecond electric discharges in gases. *Soviet Physics Uspekhi*, 15(3):282–297, March 1972.

[31] L P Babich, T. V. Loiko, and L. V. Tarasova. The physics of high-voltage nanosecond discharges in dense gases. *Radiophysics and Quantum Electronics*, 20(4):436–442, April 1977.

[32] Leonid P Babich, T V Loĭko, and V A Tsukerman. High-voltage nanosecond discharge in a dense gas at a high overvoltage with runaway electrons. *Soviet Physics Uspekhi*, 33(7):521–540, July 1990.

[33] C. a. Fenstermacher. Electron-Beam-Controlled Electrical Discharge as a Method of Pumping Large Volumes of CO2 Laser Media at High Pressure. *Applied Physics Letters*, 20(2):56, 1972.

[34] R O Hunter. Electron beam controlled switching. In *International Pulsed Power Conference*, pages IC8–1 –IC8–6, New York, NY, 1976. Institute of Electrical Engineers, Inc.

[35] B M Koval'chuk and G A Mesyats. Rapid cutoff of a high current in an electron-beam-excited discharge. *Soviet Technical Physics Letters*, 2(252), 1976.

[36] a. Jay Palmer. A physical model on the initiation of atmospheric-pressure glow discharges. *Applied Physics Letters*, 25(3):138, 1974.

[37] Jeffrey I. Levatter and Shao-Chi Lin. Necessary conditions for the homogeneous formation of pulsed avalanche discharges at high gas pressures. *Journal of Applied Physics*, 51(1):210, 1980.

[38] L M Vasilyak, S V Kostyuchenko, N N Kudryavtsev, and I V Filyugin. Fast ionisation waves under electrical breakdown conditions. *Physics-Uspekhi*, 37(3):247–268, March 1994.

[39] B B Slavin and P I Sopin. Breakdown of a neutral gas by ionizing waves of the gradient of a negative potential. *High Temperature1*, 30(1):1–9, 1992.

[40] S M Starikovskaia, N B Anikin, S V Pancheshnyi, D V Zatsepin, and A Yu Starikovskii. Pulsed breakdown at high overvoltage: development, propagation and energy branching. *Plasma Sources Science and Technology*, 10(2):344–355, May 2001.

[41] S M Starikovskaia and A Yu Starikovskii. Numerical modelling of the electron energy distribution function in the electric field of a nanosecond pulsed discharge. *Journal of Physics D: Applied Physics*, 34(23):3391–3399, December 2001.

[42] Sergey V. Pancheshnyi, Deanna A. Lacoste, Anne Bourdon, and Christophe O. Laux. Ignition of Propane–Air Mixtures by a Repetitively Pulsed Nanosecond Discharge. *IEEE Transactions on Plasma Science*, 34(6):2478–2487, December 2006.

[43] S M Starikovskaia. Plasma assisted ignition and combustion. *Journal of Physics D: Applied Physics*, 39(16):R265–R299, August 2006.

[44] Igor V. Adamovich, Walter R. Lempert, Munetake Nishihara, J. William Rich, and Yurii G. Utkin. Repetitively Pulsed Nonequilibrium Plasmas for Magnetohydrodynamic Flow Control and Plasma-Assisted Combustion. *Journal of Propulsion and Power*, 24(6):1198–1215, November 2008.

[45] S.O. Macheret, M.N. Shneider, and R.B. Miles. Modeling of air plasma generation by repetitive high-voltage nanosecond pulses. *IEEE Transactions on Plasma Science*, 30(3):1301–1314, June 2002.

[46] Steven J Schneider, Hani Kamhawi, and Isaiah M Blankson. Efficient Ionization Investigation for Flow Control and Energy Extraction. *AIAA 47th Aerospace Sciences Meeting*, 2009.

[47] A Yu Starikovskii, A A Nikipelov, M M Nudnova, and D V Roupassov. SDBD plasma actuator with nanosecond pulse-periodic discharge. *Plasma Sources Science and Technology*, 18(3):034015, August 2009.

[48] Igor V Adamovich, Munetake Nishihara, Inchul Choi, Mruthunjaya Uddi, and Walter R Lempert. Energy coupling to the plasma in repetitive nanosecond pulse discharges. *Physics of Plasmas*, 16(11):113505, 2009.

[49] Dmitry S. Nikandrov, Lev D. Tsendin, Vladimir I. Kolobov, and Robert R. Arslanbekov. Theory of Pulsed Breakdown of Dense Gases and Optimization of the Voltage Waveform. *IEEE Transactions on Plasma Science*, 36(1):131–139, 2008.

[50] H Ayan, D Staack, G Fridman, A Gutsol, Y Mukhin, A Starikovskii, A Fridman, and G Friedman. Application of nanosecond-pulsed dielectric barrier discharge for biomedical treatment of topographically non-uniform surfaces. *Journal of Physics D: Applied Physics*, 42(12):125202, June 2009.

[51] J L Zimmermann, T Shimizu, H-U Schmidt, Y-F Li, G E Morfill, and G Isbary. Test for bacterial resistance build-up against plasma treatment. *New Journal of Physics*, 14(7):073037, July 2012.

[52] John E. Foster, Grigory Adamovsky, Sarah Nowak Gucker, and Isaiah M. Blankson. A Comparative Study of the Time-Resolved Decomposition of Methylene Blue Dye Under the Action of a Nanosecond Repetitively Pulsed DBD Plasma Jet Using Liquid Chromatography and Spectrophotometry. *IEEE Transactions on Plasma Science*, 41(3):503–512, March 2013.

[53] K H Becker, U Kogelschatz, K H Schoenbach, and R J Barker. *Non-Equilibrium Air Plasmas at Atmospheric Pressure*. Institute of Physics Publishing, Bristol, UK, 2005.

[54] Guillaume Pilla, David Galley, Deanna a. Lacoste, Franois Lacas, Denis Veynante, and Christophe O. Laux. Stabilization of a Turbulent Premixed Flame Using a Nanosecond Repetitively Pulsed Plasma. *IEEE Transactions on Plasma Science*, 34(6):2471–2477, December 2006.

[55] Munetake Nishihara, J. William Rich, Walter R Lempert, Igor V Adamovich, and Sivaram Gogineni. Low-temperature M=3 flow deceleration by Lorentz force. *Physics of Fluids*, 18(8):086101, 2006.

[56] Ainan Bao, Yurii G. Utkin, Saurabh Keshav, Guofeng Lou, and Igor V. Adamovich. Ignition of Ethylene–Air and Methane–Air Flows by Low-Temperature Repetitively Pulsed Nanosecond Discharge Plasma. *IEEE Transactions on Plasma Science*, 35(6):1628–1638, December 2007.

[57] Guofeng Lou, Ainan Bao, Munetake Nishihara, Saurabh Keshav, Yurii G Utkin, J William Rich, Walter R Lempert, and Igor V Adamovich. Ignition of premixed hydrocarbon–air flows by repetitively pulsed, nanosecond pulse duration plasma. *Proceedings of the Combustion Institute*, 31(2):3327–3334, January 2007.

[58] David Z Pai, Gabi D Stancu, Deanna a Lacoste, and Christophe O Laux. Nanosecond repetitively pulsed discharges in air at atmospheric pressure—the glow regime. *Plasma Sources Science and Technology*, 18(4):045030, November 2009.

[59] Yvette Zuzeek, Inchul Choi, Mruthunjaya Uddi, Igor V Adamovich, and Walter R Lempert. Pure rotational CARS thermometry studies of low-temperature oxidation kinetics in air and ethene–air nanosecond pulse discharge plasmas. *Journal of Physics D: Applied Physics*, 43(12):124001, March 2010.

[60] Munetake Nishihara, Keisuke Udagawa Takashima, John R. Bruzzese, Igor V. Adamovich, and Datta Gaitonde. Experimental and Computational Studies of Low-Temperature Mach 4 Flow Control by Lorentz Force. *Journal of Propulsion and Power*, 27(2):467–476, March 2011.

[61] Tsuyohito Ito, Dirk Luggenhölscher, Kazunobu Kobayashi, Sarah Müller, Uwe Czarnetzki, and Satoshi Hamaguchi. Electric field measurement in an atmospheric or higher pressure gas by coherent Raman scattering of nitrogen. *Journal of Physics D: Applied Physics*, 42(9):092003, May 2009.

[62] Osaka University) Ito, Tsuyohito (Frontier Research Base For Global Young Researchers, Osaka University) Kobayashi, Kazunobu (Center For Atomic And Molecular Technologies, Ruhr-University Bochum) Czarnetzki, Uwe (Institute For Plasma And Atomic Physics, and Osaka University) Hamaguchi, Satoshi (Center For Atomic And Molecular Technologies. Rapid formation of electric field profiles in repetitively pulsed high-voltage high-pressure nanosecond discharges. *Journal of Physics D: Applied Physics*, 43(6):062001, February 2010.

[63] Sarah Müller, Dirk Luggenhölscher, and Uwe Czarnetzki. Ignition of a nanosecond-pulsed near atmospheric pressure discharge in a narrow gap. *Journal of Physics D: Applied Physics*, 44(16):165202, April 2011.

[64] S. O. Macheret, M. N. Shneider, and R. C. Murray. Ionization in strong electric fields and dynamics of nanosecond-pulse plasmas. *Physics of Plasmas*, 13(2):023502, 2006.

[65] M. Laroussi and X. Lu. Room-temperature atmospheric pressure plasma plume for biomedical applications. *Applied Physics Letters*, 87(11):113902, 2005.

[66] XinPei Lu and Mounir Laroussi. Dynamics of an atmospheric pressure plasma plume generated by submicrosecond voltage pulses. *Journal of Applied Physics*, 100(6):063302, 2006.

[67] Ulrich Kogelschatz. Dielectric-Barrier Discharges: Their History, Discharge Physics, and Industrial Applications. *Plasma Chemistry and Plasma Processing*, 23(1):1–46, 2003.

[68] J. L. Walsh, J. J. Shi, and M. G. Kong. Submicrosecond pulsed atmospheric glow discharges sustained without dielectric barriers at kilohertz frequencies. *Applied Physics Letters*, 89(16):161505, 2006.

[69] J L Walsh, D X Liu, F Iza, M Z Rong, and M G Kong. Contrasting characteristics of sub-microsecond pulsed atmospheric air and atmospheric pressure helium–oxygen glow discharges. *Journal of Physics D: Applied Physics*, 43(3):032001, January 2010.

[70] G V Naidis. Modelling of streamer propagation in atmospheric-pressure helium plasma jets. *Journal of Physics D: Applied Physics*, 43(40):402001, October 2010.

[71] Doug Breden, Kenji Miki, and Laxminarayan L. Raja. Computational study of cold atmospheric nanosecond pulsed helium plasma jet in air. *Applied Physics Letters*, 99(11):111501, 2011.

[72] Keisuke Takashima, Igor V. Adamovich, Zhongmin Xiong, Mark J. Kushner, Svetlana Starikovskaia, Uwe Czarnetzki, and Dirk Luggenhölscher. Experimental and modeling analysis of fast ionization wave discharge propagation in a rectangular geometry. *Physics of Plasmas*, 18(8):083505, 2011.

[73] Michael A. Lieberman and Allan J. Lichtenberg. *Principles of Plasma Discharges and Materials Processing*. John Wiley & Sons, Inc., Hoboken, NJ, USA, 2nd edition, April 2005.

[74] A. E. Siegman. *Lasers*. University Science Books, Sausalito, CA, 1986.